ingegneria sismica
International Journal of Earthquake Engineering
Anno XLIII - Num. 1 - 2026

Adaptability and transformation enhancement strategy of substation three-dimensional design model operation and maintenance under digital transformation environment

Youhui Chen[1,*], *Zhonghua Lü*[1], *Qi Pan*[1] *and Xinying Zhao*[1]

[1] State Grid Liaoning Electric Power Company Limited Economic Research Institute, Shenyang, Liaoning, 110015, China

SUMMARY: *The traditional substation operation and maintenance model is facing challenges such as data dispersion, response lag, and low 3D visualization. The 3D reality interaction system becomes the key to break the situation. By analyzing the standard model library, the study generates a point cloud uniformly and randomly in the triangular grid of basic elements, and then assembles it into a complete component model based on the transformation matrix. OPTICS clustering algorithm is used to segment the complex distribution of point clouds of buildings in the scene. And the integration of Web front-end technology, BIM modeling and operation and maintenance strategy optimization, to build a three-dimensional reality interactive system, to achieve equipment status visualization and inspection path planning. Under the harsh condition of point cloud thinning to 50%, the model coverage rate can still maintain 74.20%. The triangulated point cloud + OPTICS clustering in this paper significantly outperforms PCA+KNN and RANSAC+ICP with an average recognition time of 6.07 s and an accuracy of 96.73%, and the recognition accuracy shows stronger anti-interference ability under the interference of added noise and uneven density, with a noise variance of 0.08, which still reaches 55.68%. The average frame rate of 3D model rendering reaches 39.94 fps, running smoothly and stably. In actual operation and maintenance tasks, the system improves the efficiency of operations such as "running to cold standby" by 39% to 52%.*

KEYWORDS: *3D reality interactive operation and maintenance; point cloud data; OPTICS; BIM modeling; substation*

1 Introduction

The country's economy needs the stable support of the electric power industry, and as the total demand for electricity continues to increase, the development of electric power production needs to be accelerated [1]. The substation is the core content of the power system, which can combine all the power grids at different levels through the transformer, implement the voltage modification and control, receive the electric energy and rationalize the arrangement of that electric energy [2-4].

In the past, the design of the substation is commonly used in a two-dimensional way, which is less intuitive, and with the increase in the difficulty of grid construction and the increasingly fierce competition in design, this design method has been difficult to meet the diversified requirements of the current power grid project [5, 6]. It is necessary to adopt more advanced technology to solve the many factors involved in substation design, construction and operation,

*chenyouhui06@163.com
https://doi.org/10.65102/is2026058
Published: 30 April, 2026

and improve the design level and service quality.

In contrast, three-dimensional design can not only significantly improve the efficiency of designers, but also provide a more intuitive and easy to understand visualization model for construction personnel, which is not only the inevitable demand for the development of grid intelligence, but also the inevitable trend of the times [7-10]. In this context, the substation three-dimensional design model as a comprehensive information carrier, it is not only the restoration of the appearance, but also the integration of multi-dimensional information such as equipment parameters, alignment direction, space spacing, maintenance path, safety distance and so on [11-14]. However, the current model faces problems such as insufficient O&M adaptability and low transformation efficiency, and in the digital transformation environment, adopting effective strategies to enhance O&M adaptability and transformation is still an important issue for realizing efficient O&M of smart grids [15].

The research focuses on the three-dimensional reality interaction of substations, fuses the equipment state information with spatial structure, and constructs an operation and maintenance platform with both present model and arithmetic power. Starting from point cloud generation and processing, we design a method to generate point clouds uniformly and randomly within triangles by parsing the basic tuples in the standard model library. The points are randomly taken from a parallelogram face sheet, and the points falling outside the shape are folded back to the inside of the triangle through symmetry transformation, so as to quickly generate a high-coverage base point cloud. At the same time, these point clouds are assembled to form a complete device point cloud model in 3D space according to the component transformation matrix. Then, a combination of progressive morphological filtering and statistical filtering is introduced to gradually separate the ground and non-ground point clouds. The OPTICS clustering algorithm is also used, which softly divides the point cloud by two indicators, core distance and reachable distance, generates an ordered reachable map, and maintains stable segmentation effect in different density distribution areas. At the system design level, the research integrates Web front-end technology, BIM modeling platform and operation and maintenance strategy optimization algorithm to construct an interactive 3D reality system. On the one hand, through HTML5 and responsive design, cross-terminal visualization access and interactive operation are realized. On the other hand, it integrates the equipment status evaluation and warning mechanism in the background, and dynamically optimizes the inspection routes by combining the shortest path method.

2 Construction of substation operation and maintenance system based on point cloud data and three-dimensional modeling

2.1 Automated modeling for substation point cloud data

2.1.1 Construction of the model library

By analyzing the standard model library file for the parameter information of each basic element, a 3D model of the basic element can be simulated. The surface of this model is divided into several triangular and quadrilateral planes, where the quadrilateral plane is divided into two triangular planes. Within each triangular plane, we uniformly and randomly generate point clouds to generate the point cloud data of the basic atlas elements. Then, we use the rotational translation matrix to transform the basic tuples to the corresponding positions to compose the

point cloud data of the components, and finally construct the point clouds of all substation components and their 3D models.

(1) Triangulation of basic elements

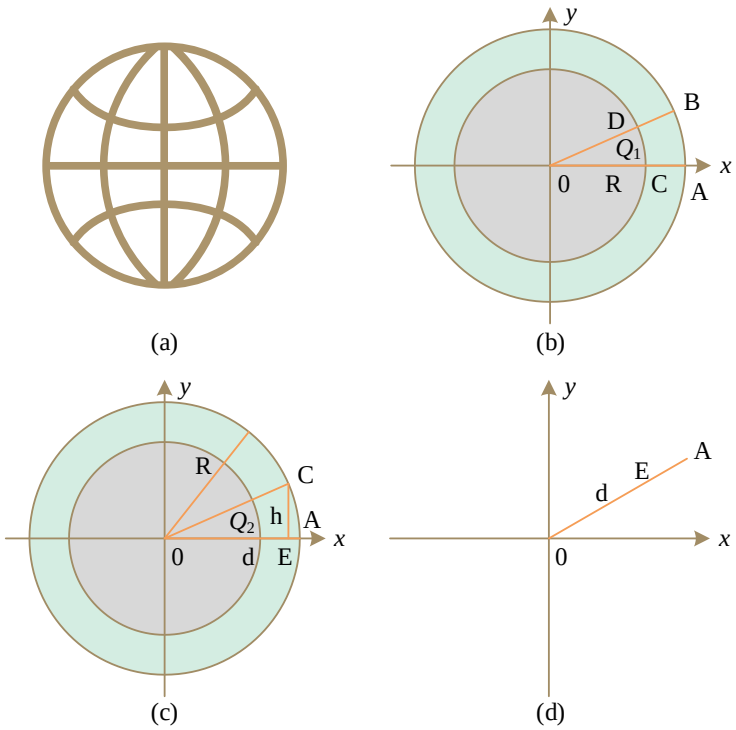

Figure 1: Analysis of Vertex Coordinates of Triangular Planes in Spherical Model

Figure 1 shows the analysis of the triangular plane vertex coordinates of the sphere model. The specification contains more than two dozen basic tuples, and each basic tuple node name is different. Take the following sphere as an example to introduce the vertex coordinate analysis method of the triangular plane of the model. The node name of the sphere model is "Sphere". The mesh of the model consists of a number of triangular and quadrilateral planes as shown in Fig. 1(a). In Fig. 1(b), the circle of the cross-section is divided into equal parts, and the angle of each part is denoted as θ_1, and from the radius R, we have $A(R,0,0)$, $B(R\cos\theta_1, R\sin\theta_1, 0)$, and the following are the coordinates of the points C and D coordinates:

Figure 1 (c) in the longitudinal section of the circle is divided into a number of equal parts, each part of the angle is recorded as θ_2, the projected point of C in the straight line OA for E, easy to obtain CE length $h = R\sin\theta_2$, OE length $d = R\cos\theta_2$, h that is, the z axis of the coordinates of the point C.

The XOY-plane after projection is shown in Fig. 1(d), noting that the coordinates of the A-point (X_A, Y_A), and the equation of the OA-line is denoted by $y = (Y_A / X_A)x$, and letting the coordinates of the E-point $E\left(X_E, (Y_A/X_A)X_E\right)$, from $X_E^2 + (Y_A^2 / X_A^2)X_E^2 = d^2$, we get the x coordinates of the E point as shown in Eqn. (1), and the y coordinates as shown in Eqn. (2):

$$X_z=\begin{cases}\sqrt{\dfrac{d^2}{1+\left(Y_A/X_A\right)^2}},\left(X_A<0\right)\\ 0,\left(X_A=0\right)\\ -\sqrt{\dfrac{d^2}{1+\left(Y_A/X_A\right)^2}},\left(X_A<0\right)\end{cases} \tag{1}$$

$$Y_z=\begin{cases}\left(Y_A/X_A\right)X_z,\left(X_A\neq 0\right)\\ d,\left(X_A=0\right)\end{cases} \tag{2}$$

where $d=R\cos\theta_2$, it is easy to know that $C\left(X_z,Y_z,R\sin\theta_2\right)$. Similarly, the coordinates of point D are obtained from the coordinates of point B. $ABCD$ constitutes a quadrangular mesh, from the above steps can be obtained from the four vertices of each quadrangular mesh, and then divided into two triangular meshes, and finally obtain the coordinates of the three vertices of all triangular meshes of the sphere model.

(2) Triangle random point taking

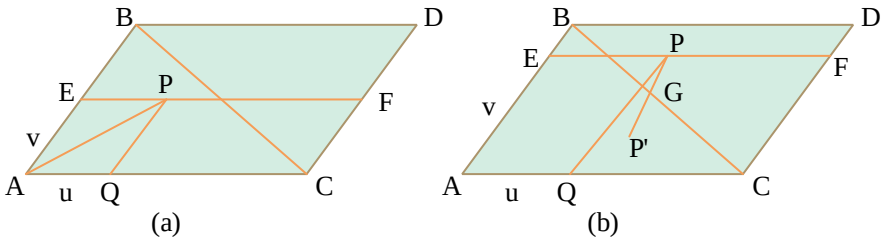

Figure 2: Analysis of random point sampling in a triangle

Figure 2 shows the analysis of random point picking in triangles. In order to generate points uniformly and randomly within each triangle, the method of quadrilateral point picking is used in this chapter. Firstly, the total area of all triangles is calculated, then the total number of point clouds is calculated based on the set density and total area, and the number of point clouds in each triangle is calculated based on the area share of each triangle. Finally, a specified number of point clouds are generated within each triangle to achieve the effect of uniform distribution. Specifically, we can take the triangle ABC in Fig. 2(a), i.e., the triangle where we need to generate random points, flip it around the side of BC to get the parallelogram $ABCD$, take an arbitrary point E on AB, take a point F on CD so that EF is parallel to AC, and take a random point P on EF. This gives us a random point. Making PQ parallel to AB over the point P gives expression (3)

$$\overrightarrow{AP}=\overrightarrow{AE}+\overrightarrow{EP} \tag{3}$$

Let $\overrightarrow{AE}=v\cdot\overrightarrow{AB}$, $\overrightarrow{EP}=\overrightarrow{AQ}=u\cdot\overrightarrow{AC}$, $\left(u,v\in\left(0,1\right)\right)$, and substituting into Eq. (3) gives Eq. (4):

$$\overrightarrow{AP}=v\cdot\overrightarrow{AB}+u\cdot\overrightarrow{AC} \tag{4}$$

The coordinates of P point are finally obtained: $P=(1-u-v)\cdot A+v\cdot B+u\cdot C$.

Since the P point may fall outside the triangle ABC, it is necessary to determine whether the P point is inside ABC. If the coefficients u or v are negative, then the P point must fall outside the parallelogram. In order for the P point to lie inside the triangle ABC, the following three conditions must be satisfied: $u>=0$, $v>=0$, and $(u+v)<=1$. Since u and v are randomly generated within $[0,1]$, it is only necessary to determine if point P is inside ABC by determining $(u+v)<=1$. If $(u+v)>1$, then the P point falls in BCD, as shown in Fig. 2(b), set the symmetry point of the P point about BC to be P', and by the centrosymmetric relationship there is the expression (5)

$$\frac{1}{2}\cdot(P+P')=G=\frac{1}{2}\cdot(B+C) \tag{5}$$

According to equation (5) we get $P'=B+C-P$.

Iterating each triangle mesh and following the above steps, the point cloud data of the basic elements of the sphere can be obtained. Similarly, the point cloud data of each basic element can be obtained.

(3) Basic Element Assembly

According to the *Transform Matrix* node in each basic element node provided in the document, each basic element point cloud can be translated and rotated according to its corresponding transform matrix, and a complete point cloud of the component is finally obtained. For the 3D mesh model of the component, the triangle planes are formed according to the coordinates of the vertices of each triangle of the basic atlas, and all the triangle planes form the 3D mesh model of the basic atlas. Then, according to the rotation translation matrix in the *Transform Matrix* node, transform operations are performed on each basic tuple model to move it to the corresponding position to form a complete mesh model of the part.

2.1.2 Extracting non-ground point clouds

When the scene point cloud is too large, it will be very inefficient to match the scene point cloud directly with the model library point cloud. In order to improve the recognition efficiency, the scene point cloud can be segmented into several modules first. These point cloud modules are individually separated in the scene except that they are connected to the ground. Therefore, the ground needs to be removed first. In this chapter, a progressive morphological filter with internal open and close operations is used to extract the ground point cloud and remove it. Next, the sparse anomaly point cloud remaining on the ground is then removed using a statistical filter. The specific steps are as follows:

(1) Read the substation point cloud data and save the x, y and z coordinates of these point cloud data in the 3D scene. Set the parameters of the algorithm, including the initial point cloud data, the window size w and the output point cloud. First, copy the initial point cloud data into the output point cloud, and make a copy of the initial point cloud at the same time. Then each point in that copy is traversed, such as the point $p_0(x_0,y_0,z_0)$, and the coordinates of the four vertices are computed based on the coordinates of the point centered within a window with width w, i.e., $(x_0-w/2,y_0-w/2)$, $(x_0+w/2,y_0-w/2)$, $(x_0-w/2,y_0+w/2)$, $(x_0+w/2,y_0+w/2)$. Add the point clouds within this window, i.e., the points that satisfy the conditions $x_0-w/2<x<x_0+w/2$ and $y_0-w/2<y<y_0+w/2$, to

an index, and get the point with the smallest z-axis coordinate in these point clouds, and replace the z-axis coordinate of the p_0 point in the output point cloud with the z-axis coordinate value of this point.

(2) After exchanging the data of the output point cloud and the copy of the point cloud, continue traversing the data of the copy of the point cloud and perform the same operation as in step 1, this time obtaining the point with the largest z-axis coordinate among all the points in the point cloud within the window range, and replace the z-axis coordinate of the point at the corresponding position in the output point cloud with the value of the z-axis coordinate of this point.

(3) Traverse all points in the initial point cloud and calculate the height difference between each point and the corresponding point in the output point cloud. Then, based on the specified height threshold, determine whether the height difference is within the threshold range. If yes, the point is categorized as a ground point cloud; otherwise, it is not taken into account.

(4) Through the above steps, we obtain the preliminary ground point cloud data and index. In order to further improve the accuracy, the window size and height threshold are appropriately increased, and several iterative operations are performed on the ground point cloud obtained in step 3 to obtain the final ground point cloud data and create the corresponding ground point cloud index.

(5) Perform an inverse operation on the ground point cloud index to obtain non-ground point cloud data. Then discrete anomalies are removed by statistical filtering:

Let a point $P_i\left(X_i, Y_i, Z_i\right)$, then the average distance between this point and its nearest k points is shown in equation (6):

$$D_i = \frac{1}{k}\sum_{j=1}^{k}\sqrt{\left(X_j - X_i\right)^2 + \left(Y_j - Y_i\right)^2 + \left(Z_j - Z_i\right)^2} \tag{6}$$

The mean value of the average distance corresponding to all points is calculated as shown in equation (7):

$$u = \frac{1}{n}\sum_{i=1}^{n} D_i \tag{7}$$

where n is the number of non-ground point cloud point clouds.

The standard deviation is shown in equation (8):

$$\sigma = \sqrt{\frac{1}{n}\sum_{i=1}^{n}\left(D_i - u\right)^2} \tag{8}$$

When the average distance D_i of the k nearest neighbors of a point P_i in the scene is within the standard range $\left(u - \delta\cdot\sigma, u + \delta\cdot\sigma\right)$, the point P_i is retained; otherwise, it is identified as an outlier and deleted. Where δ is the scale factor.

2.2 Substation building (structure) point cloud clustering

After obtaining the point cloud data, the point cloud of buildings (structures) in the substation scene needs to be effectively segmented. Since the DBSCAN algorithm is sensitive to

parameters, this section introduces the OPTICS algorithm for clustering, which realizes the orderly division of the point cloud by core distance and reachable distance.

After the power lines in the substation have been extracted and modeled, the point cloud of substation buildings located in the set G is left, and the point cloud of substation buildings should be segmented in order to facilitate the construction of three-dimensional models of substation buildings in the later stage.The DBSCAN algorithm is often used to segment the point cloud data. The DBSCAN algorithm is commonly used to segment point cloud data, but the parameters r and MinPts have a large impact on the data segmentation results of the DBSCAN algorithm. In this paper, OPTICS algorithm is used for clustering point clouds of substation buildings.

OPTICS is an improved algorithm of DBSCAN algorithm, which solves the problem that the clustering results in DBSCAN algorithm are more sensitive to the input parameters. The size of the values of the parameters r and MinPts have less influence on the clustering results of the OPTICS algorithm, so an infinite value can be assigned to the parameter r when the OPTICS algorithm is running.

The OPTICS algorithm outputs the ordered table directly after running, instead of producing direct clustering results, the data points located in the ordered table have two important attributes: core distance and reachable distance. According to the storage order of the data in the ordered table and the reachable distance can be obtained from the decision diagram, through the decision diagram can be obtained under any parameter r case of point cloud data clustering results.

Most of the concepts used in the OPTICS algorithm are the same as those in the DBSCAN algorithm, such as core points, direct density reachability, and so on. However, the OPTICS algorithm also uses concepts that do not appear in the DBSCAN algorithm: core distance and reachable distance.

Core distance: the minimum neighborhood radius that makes the current point $x \in G$ a core point is called core distance, G^1 represents the data point in the set G that is closest to the current point x, and G^i represents the data object in the set G that is the ith closest to the previous point x. The mathematical expression for core distance is shown below:

$$cd\left(x\right)=\begin{cases} undefined, & \left|N_x\right| < MinPts \\ d\left(x, G^{MinPts}\right) & \left|N_x\right| \geq MinPts \end{cases} \tag{9}$$

Reachable Distance: Let the data point $x, y \in G$, there exists a minimum distance, so that the data point x to become the core point and so that the data point y can be reached by the direct density of the data point x, this distance is known as the reachable distance, the mathematical expression is shown below.

$$rd\left(x\right)=\begin{cases} undefined, & \left|N_x\right| < MinPts \\ \max\left(cd\left(x\right), d\left(x, y\right)\right) & \left|N_x\right| \geq MinPts \end{cases} \tag{10}$$

The flow of the OPTICS algorithm to generate an ordered table is shown in Figure 3.

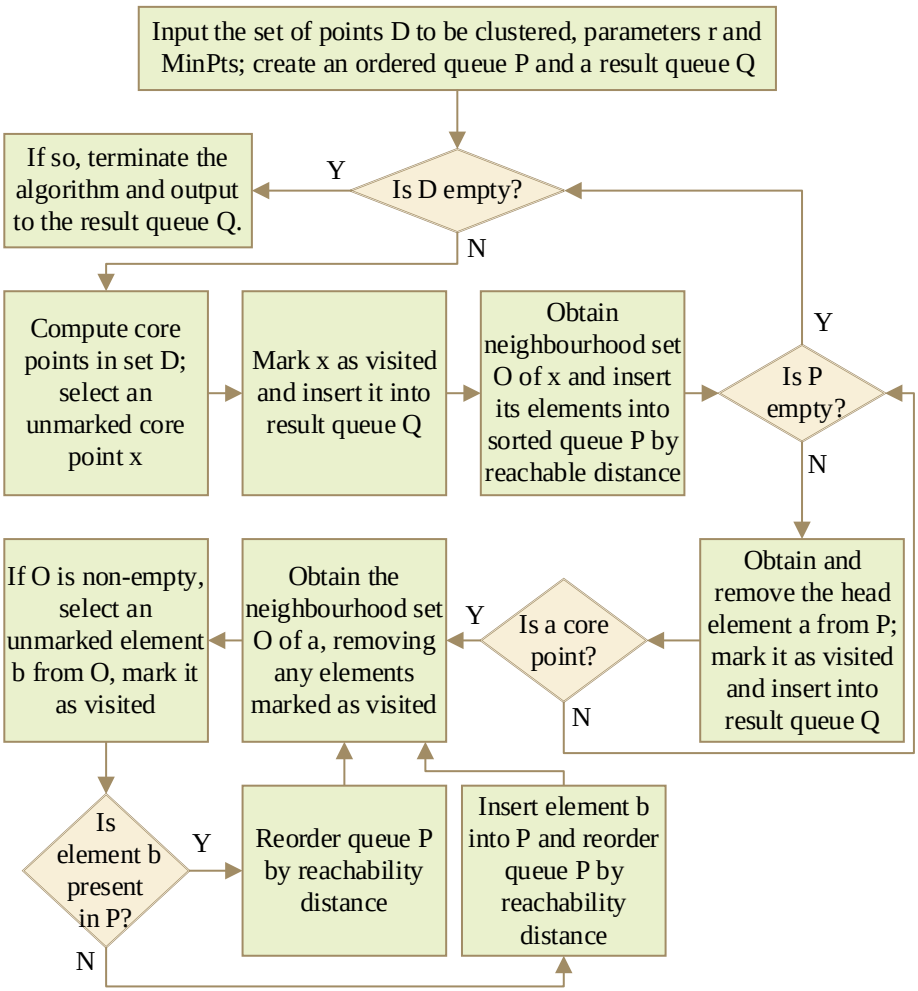

Figure 3: flow chart of generating ordered table by options algorithm

When the ordered table (result queue Q) is obtained according to the neighborhood radius r, the core distance of the data points and the reachable distance can be obtained from the final clustering results of the data objects. The specific operation process is as follows:

(1) Input the result queue Q and neighborhood radius r.

(2) Judge whether the result queue Q is empty.

(3) When the result queue is empty, the program ends and the clustering results are obtained; otherwise, a data point p of an unlabeled class cluster is randomly selected from the result queue, and it is judged whether the reachable distance of the data point p is smaller than the neighborhood radius r, and if it is smaller than that, then p is added to the current class cluster C_i; otherwise, it is compared whether the core distance of the data point p is smaller than the neighborhood radius r, and if it is smaller than that, then the new class cluster C_i is created. A new class cluster C_j and add the data point to this class cluster; otherwise the data point p is a noise point.

The OPTICS algorithm clustering algorithm is shown in Figure 4.

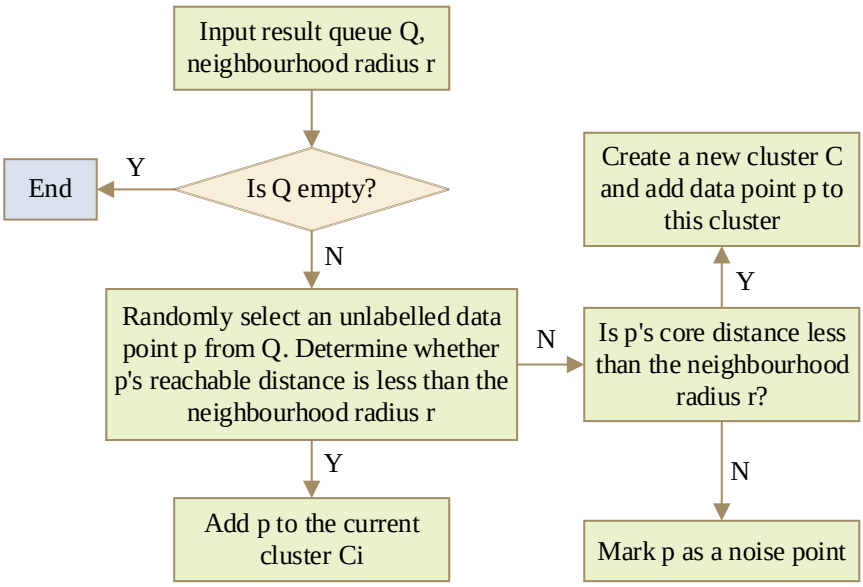

Figure 4: options clustering algorithm

2.3 Three-dimensional interactive operation and maintenance system software design

This section focuses on the front-end of the system, through the combination of Web front-end technology and BIM modeling platform, to build a 3D reality system with interactive functions.

2.3.1 Web front-end development technology substation 3D modeling

Creating Web pages with distinctive interactivity features. When developing a Web front-end to run network protocols, the overall structural layout of the page is judged through the semanticization of the Hypertext Markup Language (HTML) page structure. Selecting the appropriate semanticization tags and updating the search engine of the network can enable the equipment to accurately identify and parse the page, bringing a more ideal browsing experience to the user. The use of HTML5 can be responsive to the use of the substation scene design, so that the substation equipment operation and maintenance effects can be presented as a whole. Design front-end application web pages to enhance the interactivity between users and the interface. Relying on the interactive role of the code, a complete caching mechanism is established while the data is dynamically updated. Interactive modeling of substation 3D reality through Building Information Modeling (BIM). The geometric information of the entity is included in the model, and the full information cycle of the entity is stored. Combined with the centralized characteristics of substation equipment, AutodeskRevit is chosen as the platform to build the model.

2.3.2 Substation O&M Strategy Optimization

In order to understand the equipment operation information and equipment health status in the substation, the staff needs to grasp the operation information of the substation operation equipment in time. Collect the equipment operation status information and construct the evaluation model. According to the equipment operation and maintenance data, the operation and maintenance strategy design is carried out through the shortest path method. During the operation of substation equipment, the degree of deterioration of the equipment is described through the linear fitting method, and early warning information is issued according to the real-time status of the equipment information. Calculate the relative deterioration degree of the

equipment, and determine whether to issue warning information through the predicted value of the characteristic parameters. An electronic map of the substation is established to obtain the distribution location of different devices, and the distance between the devices is measured. The shortest path method is applied to calculate the distance between the function curve and different points, and the specific calculation formula is as follows

$$u = \sum_{i=1,\, j=1}^{n} X_{ij}\beta \tag{11}$$

where: u is the distance between the function curve and different points; n is the number of substation equipment; X is the observed value of the warning information; β is the measured value of the warning information; i and j are the coordinates of the equipment location, respectively. By quantizing this function, the best match calculation is performed on the solution based on the discrete characteristic of X. Construct the node matrix and set the distance from vertex 1 to the function curve as D_i, and the distance from vertex 2 to the function curve as D_k, when $D_i > D_k$, it means that the current path is the shortest, and if $D_i \le D_k$, it is necessary to update u, and complete the iteration when $D_i = D_k$. In this way, the shortest path between multiple points can be obtained by iteration, which makes the substation operation and maintenance strategy optimized.

3 Substation point cloud data acquisition and identification research

In Chapter 2, a full set of methods from point cloud generation, clustering processing to 3D system construction are systematically elaborated. In this chapter, a series of experiments will be carried out on the accuracy of substation point cloud data acquisition, the robustness of modeling under sparse conditions, and the performance comparison of different recognition algorithms, to verify whether the above methods can be put into practice in real-world scenarios.

3.1 Three-dimensional point cloud data acquisition accuracy test

First, to verify the accuracy of the triangle-based point cloud data acquisition method in Section 2.1, the actual spatial coordinates are compared with the points of the same name in the 3D model, and the relative error of the spatial distance between the two is calculated. During the scanning process, a certain number of control points and check points are evenly laid out and their precise geographic coordinates are measured by GPS, among which the control points are used for the conversion of the local coordinate system of the whole 3D model to the world coordinate system, and the check points are used for the accuracy check of the 3D model, i.e., to obtain the difference between the point cloud coordinates of the homonymous points and the real coordinates, and the root mean square error RMSE is used as the accuracy index.

A total of 20 check points and 20 control points were laid in this project, and the acquired coordinate information (X,Y,Z) is shown in Fig. 5.

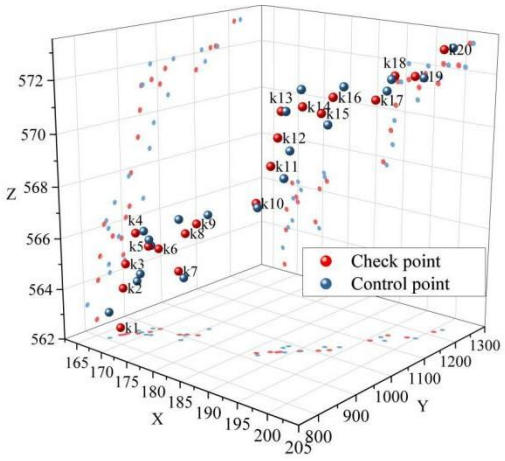

Figure 5: 20 checkpoints and 20 control point coordinate information

The homonymous points (X1,Y1,Z1) of the inspection points on the 3D model are obtained through the labeled points on the panorama, Fig. 6 shows the homonymous points based on the inspection points on the 3D model, and the three sub-figures (a), (b), and (c) show their relative errors to the actual inspection points on X, Y, and Z in the form of error bars, respectively.

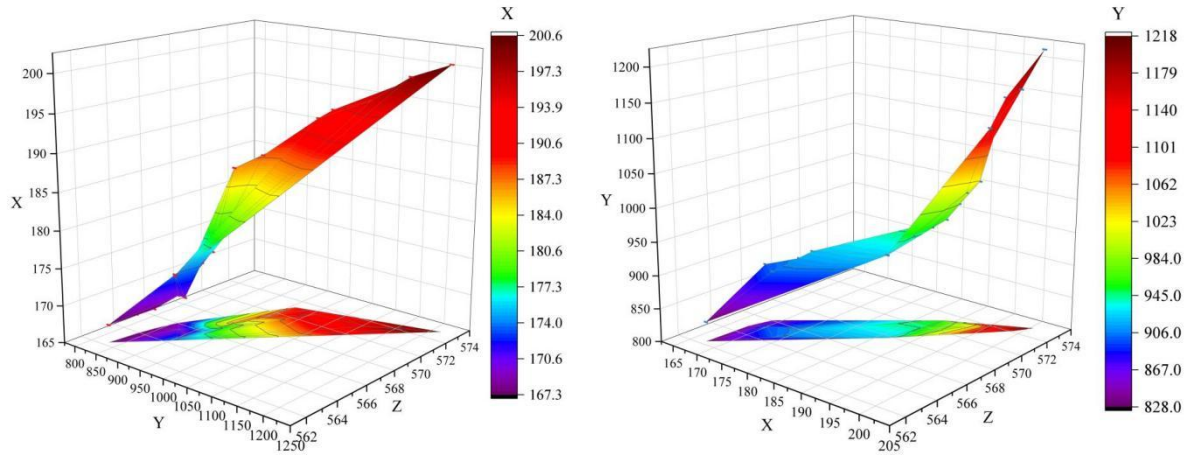

(X) (Y)

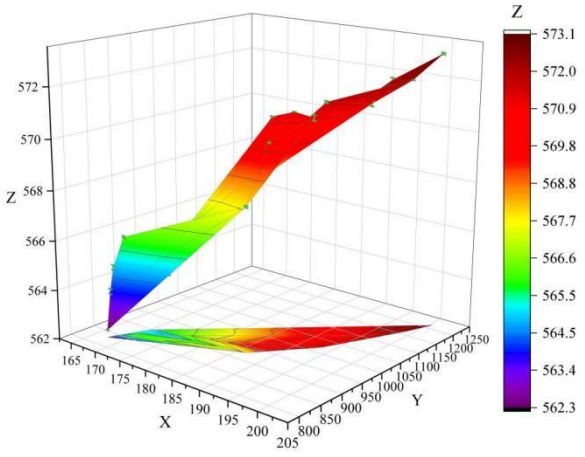

(Z)

Figure 6: Positions of the detection points on the three-dimensional model

Given that the errors are so small that it is difficult to observe the specific errors for each coordinate in Fig. 6, Fig. 7 demonstrates the relative errors for specific points on X, Y, and Z.

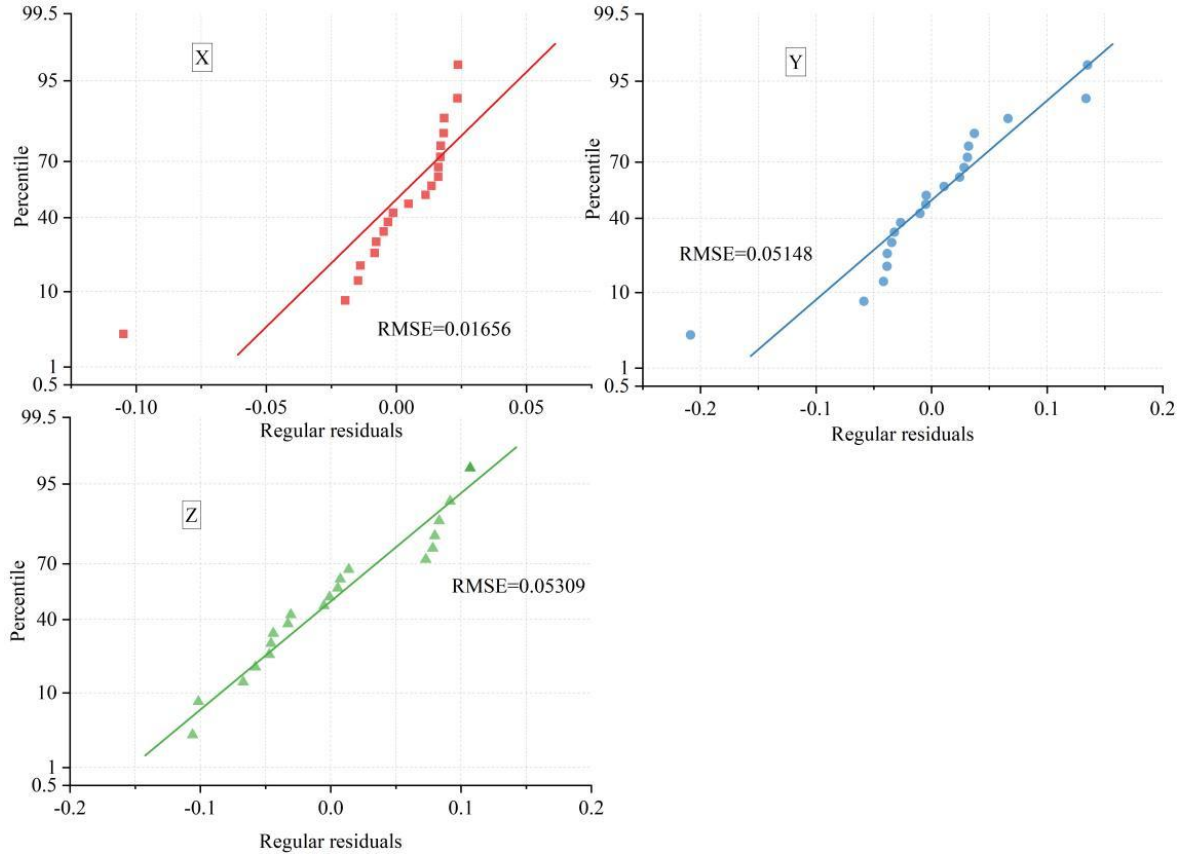

Figure 7: The relative errors of specific points on X, Y, and Z

The relative errors between the modeled and actual point locations of these 20 checkpoints are very small in the X, Y, and Z directions. The errors in the X direction are basically within ±0.02, the Y direction is slightly larger within ±0.05, and the individual points are close to 0.2 m, and in the Z direction, they are scattered approximately between [-0.1,0.1]. The final root mean square error RMSEs of the 20 points in the three directions were 0.0166, 0.0514 and 0.0531, respectively. Indicating that the methodology used in this paper to generate the point cloud by randomly picking up points from triangles and assembling them is plausible in terms of positional accuracy, especially in the horizontal direction. This automated modeling method generates models with a high degree of alignment to the actual space.

3.2 Fitting results to sparse point clouds

The above experiments were conducted with a very sufficient sample size, and to further test the robustness of the automated modeling approach for substation point cloud data in Section 2.1 under sparse point cloud samples, a point cloud sparse collection level of 5%-80% was set to assess the completeness of the modeling results based on two evaluation metrics: coverage (percentage of points within the reconstructed structural correlation) and root-mean-square error of the fit, and to measure the reconstructed geometric fidelity. The experimental results are shown in Fig. 8. The X-Y mapping represents the change of reconstruction coverage with increasing point cloud thinning, and the X-Z mapping represents the change of RMSE with increasing point cloud thinning.

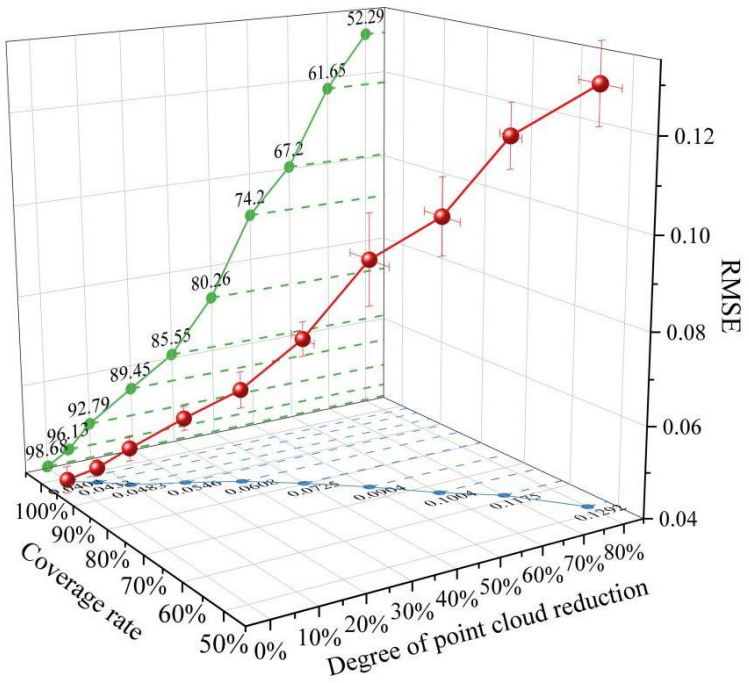

Figure 8: Coverage and RMSE under different levels of point cloud reduction

As the data become more and more sparse, the point cloud coverage gradually decreases from 98.68% to 52.29%, while the fitting error increases from 0.0404 to 0.1292. The denser the point cloud is, the more complete and accurate the reconstruction is; and the more sparse the point cloud is, the more details are lost in the model, and the error accumulates gradually. When 50% of the original data is thinned, i.e., only half of the point cloud is used, the coverage can still be maintained at 74.2%, and the error is only 0.0904. Moreover, in the first 50% of the gradual thinning, the increase of the model RMSE and the decrease of the coverage change slowly, and the equipment model can still be correctly fitted, and the accuracy is maintained at a relatively high level. It shows that the method in this paper is still robust in the face of insufficient data, and will not completely collapse because of some missing data. This is based on the design idea of uniformly distributing the points within the triangle, even if the total number of points decreases, as long as the point cloud maintains a uniform distribution within the surface, the main outline of the structure can still be outlined.

3.3 Comparison experiments of different point cloud recognition algorithms

To further verify the effectiveness of this paper's triangular extraction point cloud + OPTICS clustering method for substation point cloud recognition, two other substation equipment point cloud recognition methods are selected for comparison experiments.

Method 1 is to use PCA to obtain the local coordinate system of the equipment point cloud, then divide the point cloud space, take the cosine value of the angle between the center of gravity of the subspace and the center of gravity of the overall equipment point cloud as the feature of the subspace, and finally use the KNN algorithm to realize the recognition of the equipment point cloud.

Method 2 uses the RANSAC algorithm to extract the optimal planar features of the point cloud of the equipment to be recognized, searches for the top 5 matching templates in the template library with the features, then extracts the key points of the equipment point cloud based on the curvature information of the point cloud, and finally uses the ICP algorithm to

carry out the accurate matching to realize the recognition of the substation equipment.

3.3.1 Comparison of time-consuming and accuracy of point cloud recognition by different devices

The study selects 153 point clouds of devices to be recognized and 67 sets of template data, and the experimental results under the three recognition methods are shown in Figures 9, 10 and 11, respectively. The vertical coordinate recognition 1 is accurate recognition and 0 is recognition failure.

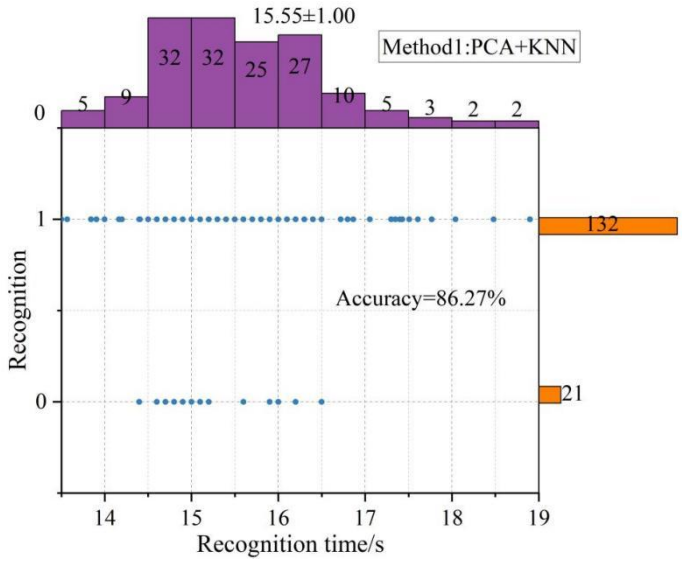

Figure 9: Point cloud recognition time and accuracyof Method 1

Based on PCA+KNN method 1, the recognition time is concentrated in the interval of [14.5,17], and there even exist 12 point cloud samples with recognition time more than 17s, and 132 samples are accurately recognized, and 21 samples are still not accurately recognized. This is because using PCA to establish the local coordinate system of the device point cloud cannot distinguish the position of the device point cloud when the coordinate axes are close together, so the recognition accuracy is low, only 86.27%.

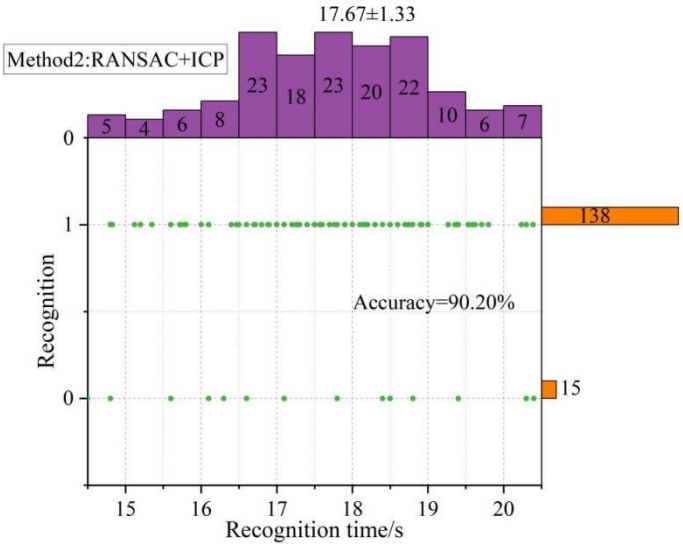

Figure 10: Point cloud recognition time and accuracyof Method 2

The average recognition time of the RANSAC+ICP-based method 2 for 152 point cloud samples averages 17.67±1.33s, which is the longest, due to the fact that the algorithm needs to extract the optimal planar features of the device point cloud by using the RANSAC iteratively, and it also needs to compute the curvature of each point for the extraction of the key points, and finally, it needs to use the ICP algorithm for each pre-selected model to accomplish the Finally, the ICP algorithm is used for each pre-selected model to complete the accurate recognition of the device point cloud, so the algorithm takes a long time. Its recognition accuracy is improved compared with the PCA+KNN method1, which accurately recognizes 138 samples with an accuracy of 90.20%.

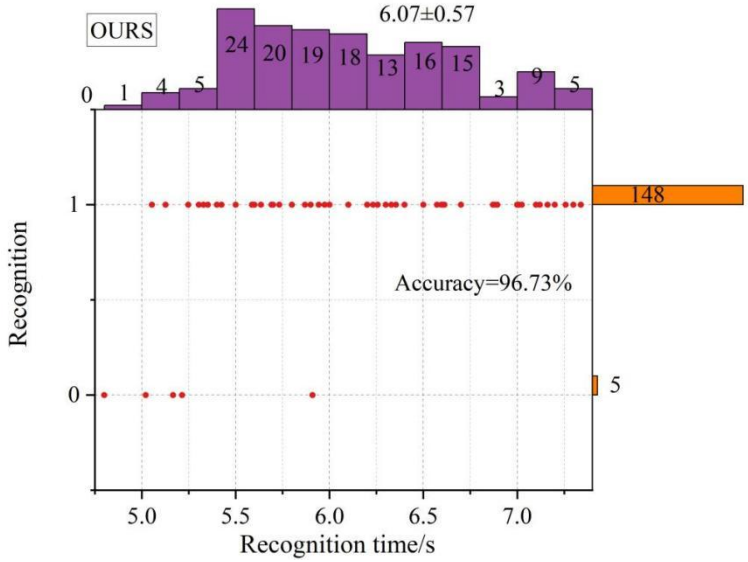

Figure 11: Point cloud recognition time and accuracyof OURS

This paper's method is optimal in both recognition efficiency and accuracy. In terms of recognition time, this paper's method takes only 6.07 seconds on average, which is less than half of the other two commonly used methods (15.55s and 17.67s), and the majority of the samples (125) are clustered in the interval of [5.5,6.75]. And only 5 samples were not accurately recognized with 96.73% accuracy, ahead of 86.27% for PCA+KNN and 90.20% for RANSAC+ICP. The spatial distribution of the regular point cloud generated by triangular homogeneous point picking has a better differentiation itself, and then segmented by OPTICS clustering, which reduces the dependence on local features in the recognition. This makes the method in this paper maintain high accuracy and improve processing speed at the same time.

3.3.2 Noise in the point cloud

To further test the robustness of the device point cloud recognition method proposed in this paper when the device point cloud has noise and uneven point cloud density, Gaussian noise with different standard deviation σ was continued to be added to 152 device point clouds to be recognized. Figure 12 shows the comparison of different device point cloud recognition algorithms in the presence of noise in the point cloud.

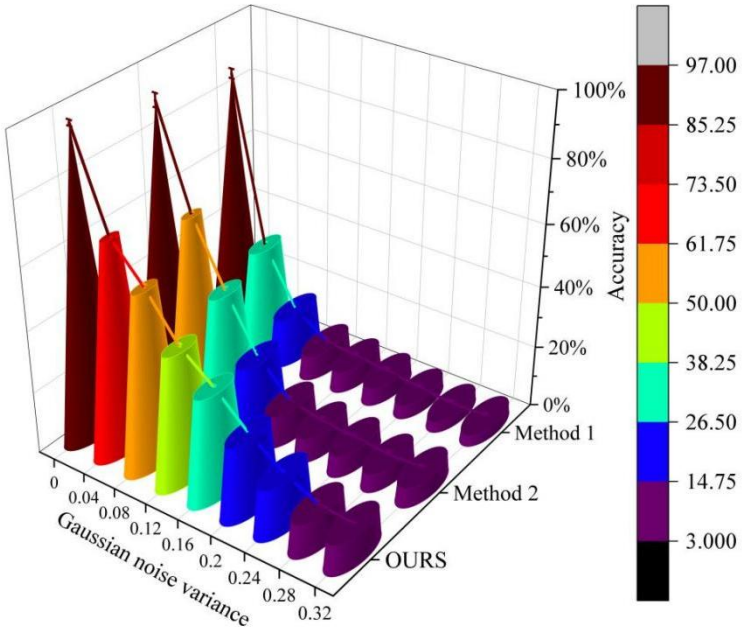

Figure 12: Comparison of different algorithms of point cloud recognition under noise

When Gaussian noise is added to the point cloud, the accuracy of all the methods declines, but this paper's method still maintains a recognition rate of 55.68% at a noise variance of 0.08, while the other two methods have dropped to 15.16% and 38.07%. It shows that the method in this paper is more resilient in the noise environment. This paper is based on the triangular uniform point picking, which essentially maintains the structural integrity at the grid level, and the noise points, although they will disturb the local position, are less likely to change the overall distribution pattern of the point cloud, coupled with the fact that the OPTICS clustering does not rely on a strict neighborhood threshold, which is better adapted to the presence of interference in the data distribution. The combination of the two makes the recognition process less likely to be biased by random noise, reflecting better structure preservation ability. When the number of noise points increases, the local coordinate system established by method 1 based on PCA will be inaccurate and the obtained subspace feature vectors will be greatly changed. And method 2 based on planar features cannot preselect the real template for processing when the noise is large, which leads to recognition error.

3.3.3 Uneven point cloud density

In order to simulate the uneven point cloud density caused by sampling, 152 device point cloud objects are layered along the z-axis at 0.5m intervals, and then voxel downsampling is used in each layer by setting the downsampling voxel size of layer 0 to d_0 and the downsampling voxel size of layer i to $d_0 * i$, and different degrees of downsampling are applied to the device point clouds by setting different d_0. Figure 13 shows the comparison of different device point cloud recognition algorithms when the point cloud density is not uniform.

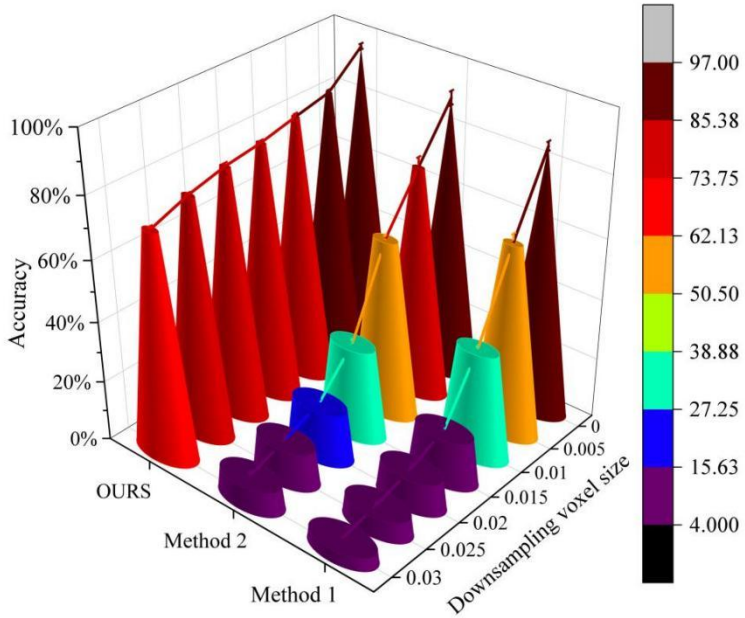

Figure 13: Accuracy of different algorithms of uneven point cloud density

As the degree of hierarchical downsampling intensifies, the recognition rates of all three methods are decreasing, but the decline curve of the method in this paper is obviously much flatter, and even when the size of downsampled voxels reaches 0.03, it still maintains an accuracy of 72.59%, while the other two methods are already less than 10%. When the density of the device point cloud is not uniform, the overall point cloud center of gravity will be severely shifted. Method 1 based on PCA+KNN uses the cosine value of the angle between the center of gravity of the subspace and the line connecting the center of gravity of the overall point cloud as the feature of the subspace, and thus is very sensitive to the density of the point cloud, which will result in the computed features not having the ability to characterize the point cloud of the device. Method 2 uses the RANSAC algorithm to extract planar features, while the planar features have only four parameters, the quality of the point cloud to be recognized requires high quality, and when the density of the point cloud is not uniform, it is impossible to accurately extract the planar features, which leads to a decrease in the recognition accuracy. In contrast, the method in this paper adopts the logic of uniformly distributing points within a triangle, even if the overall point cloud density is not uniform, as long as the distribution of points on each local triangular surface is uniform, the structural expression of that local region can be maintained. At the same time, OPTICS clustering is also insensitive to density variations, which relies on the reachability relationship between points rather than the absolute density. Therefore, in the face of unevenly sparse and dense data, the method in this paper is still able to capture the main structural features, and will not fail completely just because the points become fewer in some regions.

4 Performance verification and application effect analysis of 3D reality interactive operation and maintenance system

After verifying the feasibility and advantages of the triangular extraction point cloud + OPTICS clustering method for identifying point cloud recognition, the method is integrated into the 3D reality interactive operation and maintenance system. Chapter 4 focuses on the overall performance of the system and the effect of O&M optimization, and conducts a comprehensive

evaluation from two dimensions: the smoothness of model rendering and the efficiency improvement of interactive operation.

4.1 Comparison of model rendering effects

Now gathered into the research comparison of 3D modeling system, in order to verify the application effect of the 3D reality system constructed based on Web front-end, BIM modeling and O&M strategy optimization proposed in Section 2.3 of this paper, the model frame rate is selected as an index to evaluate the rendering smoothness. And the three methods of substation modeling with 3D laser scanning point cloud data, 3D modeling method of substation equipment with improved ORB-SLAM, and secondary equipment modeling method (SE) for substation digital design are used as comparison methods. By comparing the change of frame rate index value in the process of rendering model of each method, the smoothness of model rendering by this paper's method is analyzed, so as to verify the model rendering effect of this paper's method.

Figure 14 shows the frame rates of substation visualization models constructed under different methods recorded every 10s for 5 minutes, each method contains 30 data points each.

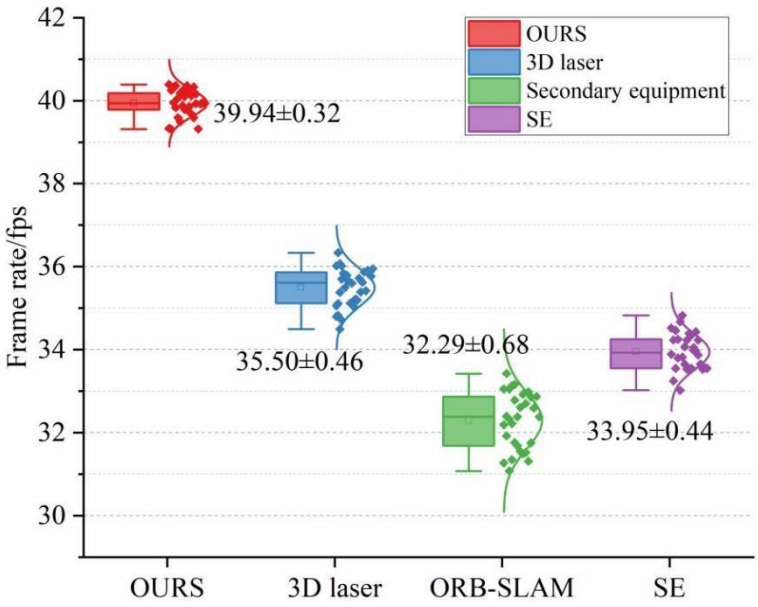

Figure 14: Frame rates of substation visualization models under different methods

The substation visualization model constructed by this paper's method is quite outstanding in terms of rendering smoothness, the average frame rate of 30 data points reaches 39.94 fps, and the frame rate fluctuation error is only 0.32, the minimum and maximum data points are 39.31 and 40.39 respectively, which indicates that the rendering process is very stable, almost no lag, and at the same time, it has a high degree of smoothness. The average frame rate of 3D laser scanning point cloud data, improved ORB-SLAM and secondary device-based modeling are 35.50±0.46, 32.29±0.68 and 33.95±0.44 fps, respectively, and the fluctuation of the frame rate is much larger in these three methods, and the change of data points is even as high as 2 fps within 5 minutes. To modeling, but adopts a lightweight path of Web front-end and BIM integration. On the one hand, with HTML5 and responsive design, the system can schedule graphic resources more efficiently; on the other hand, based on the structured model data of BIM, the rendering does not need to carry out a lot of point cloud computation in real time, which greatly improves the frame rate and stability.

4.2 Interactive O&M System Optimization Effects

In order to further verify the advantages of this paper's O&M strategy optimization over the traditional O&M system, the tasks under 220kV and 110kV are selected, and the tasks are operated with this paper's substation interactive O&M system and the traditional O&M system respectively, and the time consumed by both is compared.

Eight operation tasks are selected: operation to hot standby, hot standby to operation, operation to cold standby, cold standby to operation, operation to switch maintenance, switch inspection and modification of operation, operation to line inspection and modification of operation, and line inspection and modification of operation. A comparison of the efficiency of 220 kV and 110 kV line outage and reactivation operations under the two systems is shown in Figure 15.

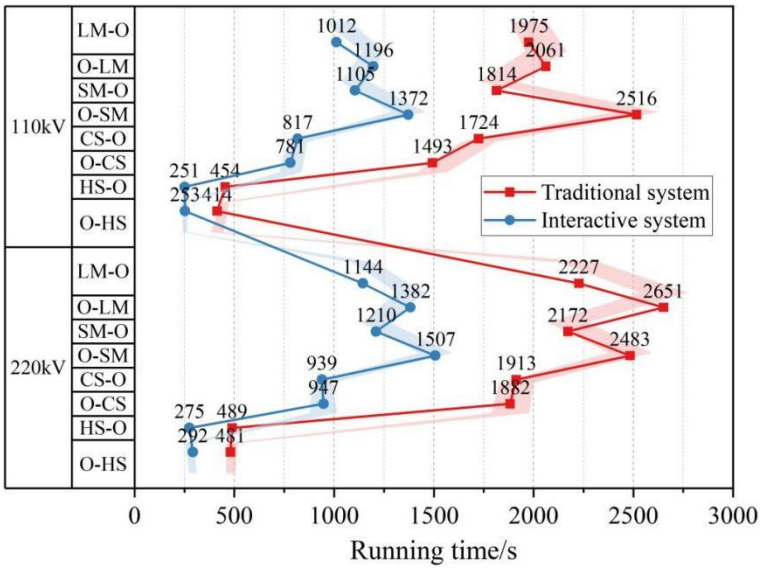

Figure 15: Efficiency of 2 operational systems under 220kV and 110-kV lines

Figure 15 clearly shows the efficiency dividend brought by the optimization of operation and maintenance strategy. Whether it is 220kV or 110kV lines, in eight typical operation tasks, the interactive system in this paper realizes significant speed-up compared with the traditional way, and the efficiency improvement ranges from 39% to 52%. 220kV operation to cold standby task, the time consumed is reduced from 1882s to 947s, which is almost half of the time saved; 110kV under the same reason, cold standby to run under the task of time-consuming from 1724s prompt to 817s, saving 907s, efficiency prompt 52.61%. This paper proves that the operation and maintenance strategy optimization mechanism of the first, through the electronic map positioning equipment, based on the shortest path dynamic planning inspection routes, to help operation and maintenance personnel less errands, fast positioning. Traditional O&M relies on manual memory and on-site groping, while the system in this paper digitally associates equipment location, state topology and operation logic, making the task execution path clear and visible, and significantly reducing non-essential time loss.

5 Conclusion

The research focuses on the actual needs of three-dimensional operation and maintenance of substations, forming a complete path from data identification to system integration, with advantages in accuracy, efficiency, robustness and practicality, which not only performs well at

the visualization level, but also substantially assists in decision-making and optimization of processes.

(1) In this paper, based on the method of triangular uniform point distribution and component assembly, the automated generated point cloud fits well with the actual measurement values, and the root-mean-square error of the coordinates is only centimeter-level, which is 0.0166m, 0.0515m, and 0.0531m in the X, Y, and Z directions, respectively.

(2) Even in the extreme case where the point cloud data are thinned to 80%, the model structure coverage still reaches 52.29%.

(3) In the test of 153 device point clouds, the average time of this method is only 6.07s, with an accuracy of 96.73%, which is 12.12% and 7.24% higher than the 86.27% and 90.20% of PCA+KNN and RANSAC+ICP, respectively.

(4) When Gaussian noise is added to simulate realistic interference, the recognition accuracy of this method still reaches 67.03% at σ=0.04, which maintains at the usable level and is much higher than that of the comparison methods at 33.29% and 58.71%, showing stronger environmental adaptability.

(5) When the density of point cloud is uneven, the recognition rate of this method still reaches 72.59% even when the downsampled voxel = 0.03, while the PCA+KNN and RANSAC+ICP methods only reach 4.07% and 7.86% at this time.

(6) In this paper, the fusion of Web front-end, BIM and O&M strategy optimization system, the rendering frame rate of 30 data points in 5 minutes is stable at about 39.94fps, and the fluctuation error is very small, only 0.32, which is better than other modeling methods.

(7) At the level of O&M efficiency, the system reduces the average time consumed for typical operation tasks such as running change cold standby by about 40%-52% by integrating e-map and shortest path planning, in which the time consumed for 220kV line-related tasks is reduced from 1882s to 947s, with an efficiency improvement of 49.68%.

Funding

This work was supported by the Management Science and Technology Project of State Grid Liaoning Electric Power Co., Ltd.(Fund Project: Research on the Adaptability and Transformation Enhancement Strategy of Substation 3D Design Model in Operation and Maintenance Scenario (Project Number:2023YF-75)).

About the Author

Youhui Chen (1987.11-), female, Han ethnicity, from Siping, Jilin. She graduated with a Master's degree in Structural Engineering from Northeast Electric Power University and currently works as a senior engineer in the Design Center Department of State Grid Liaoning Electric Power Company Limited Economic Research Institute's Technical and Economic Research Institute. Her main research direction is line structure review.

Zhonghua Lü, male, Han ethnicity, born December 24, 1976, in Dandong, Liaoning Province. Bachelor's degree holder and Senior Engineer. He is currently employed at the Economic and Technical Research Institute of State Grid Liaoning Electric Power Company Limited Economic Research Institute. His main research direction is power transmission and transformation design review.

Qi Pan (1988.4-),female, Han nationality, from Yingkou, Liaoning Province, graduated from the University of Manchester in the United Kingdom with a master's degree in electrical engineering and automation. She is now a senior engineer in the design center department of

the State Grid Liaoning Electric Power Company Limited Economic Research Institute, and her main research direction is transmission lines.

Xinying Zhao was born in Yingkou, Liaoning, China in 1996. She obtained a master's degree from Northeastern University in China. She is currently employed at the Economic and Technical Research Institute of State Grid Liaoning Electric Power Company Limited Economic Research Institute. Her main research direction is the design of power transmission and transformation projects.

References

[1] Hasanuzzaman, M., Zubir, U. S., Ilham, N. I., & Seng Che, H. (2017). Global electricity demand, generation, grid system, and renewable energy polices: a review. Wiley Interdisciplinary Reviews: Energy and Environment, 6(3), e222.

[2] Krieg, T. (2019). Substations. In Springer Handbook of Power Systems (pp. 867-934). Singapore: Springer Singapore.

[3] Huang, Q., Jing, S., Li, J., Cai, D., Wu, J., & Zhen, W. (2016). Smart substation: State of the art and future development. IEEE Transactions on Power Delivery, 32(2), 1098-1105.

[4] Ma, J., Zhu, M., Cai, X., & Li, Y. W. (2018). DC substation for DC grid—Part II: Hierarchical control strategy and verifications. IEEE Transactions on Power Electronics, 34(9), 8682-8696.

[5] Neamt, L., & Chiver, O. (2021). A simple design method of unequal spacing arrangement for substation grounding grid. IEEE Access, 9, 141339-141346.

[6] Zhang, X., & Sun, Z. (2023, April). Research on the Two-dimensional Electric Field on the Conductor Surface of 750 kV Transformer Substation under Different Structures. In Journal of Physics: Conference Series (Vol. 2474, No. 1, p. 012025). IOP Publishing.

[7] Xu, W., Shi, J., Sun, Z., Lv, S., Fang, J., Li, W., ... & Ni, Y. (2022, December). Research and application of forward three-dimensional design method of substation. In Journal of Physics: Conference Series (Vol. 2395, No. 1, p. 012054). IOP Publishing.

[8] Shi, X., Mi, X., Qian, W., Cao, Y., Hu, R., Liu, Y., ... & Zhu, J. (2024, August). Substation 3D Parametric Modeling Method and System Based on Engineering Design Drawings. In The Purple Mountain Forum on Smart Grid Protection and Control (pp. 812-829). Singapore: Springer Nature Singapore.

[9] Lei, C., Wu, X., Liu, G., Mao, W., Li, Y., Gan, X., ... & Shen, X. (2025, June). Expectation and status key technology of 3D model design for substation. In Second International Conference on Electronics, Electrical, and Control System (EECS 2025) (Vol. 13659, pp. 196-204). SPIE.

[10] Gao, Y. (2020, March). Application of 3D design technology in substation design. In IOP Conference Series: Materials Science and Engineering (Vol. 782, No. 3, p. 032086). IOP Publishing.

[11] Li, J., Hu, J., Shi, J., & Wang, H. (2022, October). Research on classification and coding

technology of substation engineering model based on 3D design. In 2022 Asian Conference on Frontiers of Power and Energy (ACFPE) (pp. 535-539). IEEE.

[12] Hu, J., Guan, L., Li, B., Lv, J., Yang, X., Wang, H., & Shi, J. (2020, April). In-Depth Study of Three-Dimensional Design Content of Transformer Substation. In 2020 3rd International Conference on Advanced Electronic Materials, Computers and Software Engineering (AEMCSE) (pp. 936-940). IEEE.

[13] Chen, X., Zheng, X., Xu, G., Shu, Z., Ji, Y., & Xu, C. (2024, July). A Construction Method for Three-Dimensional Digital Model of Substation Equipments Integrating Grid Information Model. In Journal of Physics: Conference Series (Vol. 2774, No. 1, p. 012040). IOP Publishing.

[14] Redmond, J. (2022, April). Revit 3D modeling optimizes substation design. In 2022 IEEE Rural Electric Power Conference (REPC) (pp. 84-87). IEEE.

[15] Xie, Q., Zhu, T., Bao, Y., Jian, X., & Li, A. (2025, April). Research on the automated process of three-dimensional modeling of substation assisted by artificial intelligence and its accuracy improvement. In Fifth International Conference on Telecommunications, Optics, and Computer Science (TOCS 2024) (Vol. 13629, pp. 735-741). SPIE.